Fuzzy Algorithm for Supervisory Voltage/Frequency Control of a Self Excited Induction Generator

Hussein F. Soliman, Abdel-Fattah Attia, S. M. Mokhymar, M. A. L. Badr

This paper presents the application of a Fuzzy Logic Controller (FLC) to regulate the voltage of a Self Excited Induction Generator (SEIG) driven by Wind Energy Conversion Schemes (WECS). The proposed FLC is used to tune the integral gain (KI) of a Proportional plus Integral (PI) controller. Two types of controls, for the generator and for the wind turbine, using a FLC algorithm, are introduced in this paper. The voltage control is performed to adapt the terminal voltage via self excitation. The frequency control is conducted to adjust the stator frequency through tuning the pitch angle of the WECS blades. Both controllers utilize the Fuzzy technique to enhance the overall dynamic performance. The simulation result depicts a better dynamic response for the system under study during the starting period, and the load variation. The percentage overshoot, rising time and oscillation are better with the fuzzy controller than with the PI controller type.

Keywords: fuzzy logic controller, self exited induction generator, voltage control, frequency control, wind power station.

1 Introduction

Many publications in the field of SEIG have been dealt with solutions to a range of problems (e.g. enhancing performance, loading, interfacing with the grid, etc). El Sousy et al [1] discuss a method for controlling a 3 phase induction generator using indirect field orientation control, while Mashaly at al [2] introduce an FLC controller for a wind energy utilization scheme. We have found no studies concentrating on a wind energy scheme system for supplying an isolated load. The primary advantages of SEIG are less maintenance costs, better transient performance, no need for dc power supply for field excitation, brushless construction (squirrel-cage rotor), etc. In addition, induction generators have been widely employed to operate as wind-turbine generators and small hydroelectric generators for isolated power systems [3, 4].

Induction generators can be connected to large power systems, in order to inject electric power, when the rotor speed of the induction generator is greater than the synchronous speed of the air-gap-revolving field. In this paper the dynamic performance is studied for SEIG driven by WECS to feed an isolated load. The d-q axes equivalent circuit model based on different reference frames extracted from fundamental machine theory can be employed to analyze the response of the machine transient in dynamic performance [3,4]. The voltage controller, for SEIG, is conducted to adapt the terminal voltage, via a semiconductor switching system. The semiconductor switch regulates the duty cycle, which adjusts the value of the capacitor bank connected to the SEIG [5, 6]. The SEIG is equipped with a frequency controller to regulate the mechanical input power. In addition, the stator frequency is regulated. This is achieved by adjusting the pitch angle of the wind turbine. In this paper, the integral gain (K_i) of the PI controller is supervised using the FLC to enhance the overall dynamics response. The simulation results of the proposed technique are compared with the results obtained for the PI with fixed and variable K_i.

2 The system under study

Fig. 1 shows the block diagram for the study system, which consists of SEIGs driven by WECS connected to an isolated

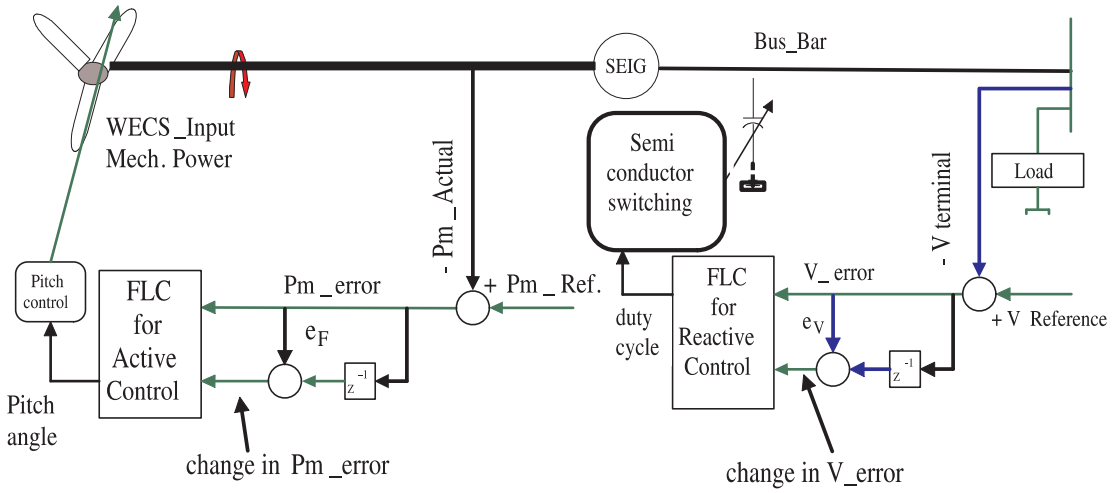

Fig. 1: System under study

load. Two control loops for terminal voltage and pitch angle using FLC to tune K_i of the PI controller are shown in the same figure. The mathematical model of SEIG driven by WECS is simulated using the MATLAB/SIMULINK package to solve the differential equations. Meanwhile, two controllers have been developed for this system. The first is the voltage controller to adjust the terminal voltage at the rated value. This is done by varying the switching capacitor bank, for changing the duty cycle, to adjust the self excitation. The second controller is the frequency controller to regulate the input power to the generator and thus to keep the stator frequency constant. This is achieved by changing the value of the pitch angle for the blade of the wind turbine. First, the system under study is tested when equipped with a PI controller for both voltage and frequency controllers at different fixed values K_I. Then the technique is developed to drive the PI controller by a variable K_I to enhance the dynamic performance of the SEIG. K_I is then tuned by using two different algorithms.

The simulation is carried out when the PI controller is driven by variable K_I using a linear function, with limitors, between K_I and voltage error for voltage control. The simulation also includes variable K_I based on the mechanical power error for the frequency controller. Meanwhile, variable K_I has lower and upper limits. Then, the simulation is conducted when the PI controller is driven by a variable K_I through FLC technique. The simulation results depict the variation of the different variables of the system under study, such as terminal voltage, load current, frequency, duty cycles of the switching capacitor bank, variable K_I in voltage controller K_{IV} and variable K_I in frequency controller K_{IF}.

3 Mathematical model of the SEIG driven by WECS

3.1 Electrical equation of the SEIG

The stator and rotor voltage equations using the Krause transformation [3, 4], based on a stationary reference frame, are given in the appendix [7].

3.2 Mechanical equations of the WECS

The mechanical equations relating the power coefficient of the wind turbine, the tip speed ratio (μ) and the pitch angle (β) are given in [7, 8, 9]. The analysis of an SEIG in this research is performed taking the following assumptions into account [3]:

- All parameters of the machine can be considered constant except X_m.
- Per-unit values of the stator and rotor leakage reactance are equal.
- Core loss in the excitation branch is neglected.
- Space and time harmonic effects are ignored.

3.3 Equivalent circuit

The d and q axes equivalent-circuit models parameters for a no-load, three-phase symmetrical induction generator refer to a 1.1 kW, 127/ 220 V (line voltage), 8.3/4.8 A (line current), 60 Hz, 2 poles, wound-rotor induction machine [4]. More details about the machine are described in [7, 8].

3.4 Voltage control and switching capacitor bank technique:

3.4.1 Switching

Switching of capacitors has been discarded in the past because of the practical difficulties involved [5, 6], i.e. the occurrence of voltage and current transients. It has been argued, and justly so, that current 'spikes', for example, would inevitably exceed the maximum current rating as well as the (di/dt) value of a particular semiconductor switch. The only way out of this dilemma would be to design the semiconductor switch to withstand the transient value at the switching instant.

The equivalent circuit in Fig. 2 is added to explain this situation of the switching capacitor bank due to the duty cycle. The details of this circuit are given in [6]. For the circuit of Fig. 2, the switches are operated in anti-phase, i.e. the switching function fs2 which controls switch S_2 is the inverse function of f_{s1} which controls switch S_1. In other words, switch S_2 is closed during the time when switch S_1 is open, and vice versa. This means that S_1 and S_2 of branch 1 and 2 are operated in such a manner that one switch is closed while the other is open.

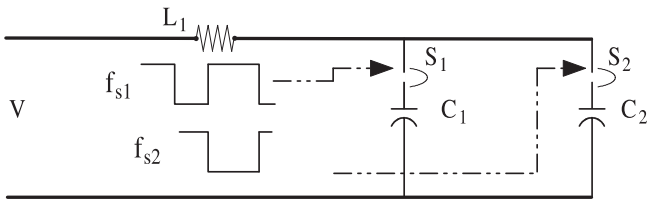

Fig. 2: Semi conductor switches (S_1, S_2) circuit for capacitor bank

3.4.2 Voltage control

As shown in Fig. 1, the input to the controllers is the voltage error, while the output of the controllers is used to execute the duty cycle (λ). The value of calculated λ is used as an input to the semiconductor switches to change the value of the capacitor bank according to the need for the effective value of the excitation. Accordingly, the terminal voltage is controlled by adjusting the self-excitation through automatic switching of the capacitor bank.

3.5 Frequency control

Frequency control is applied to the system by adjusting the pitch angle of the wind turbine blades. This is used to keep the SEIG operating at a constant stator frequency and to counteract the speed disturbance effect. The pitch angle is a function of the power coefficient C_p of the wind turbine WECS. The value of C_p is calculated using the pitch angle value according to the equation mentioned in [7, 8, 9]. Consequently, the best adjustment for the value of the pitch angle improves the mechanical power regulation, which, in turn, achieves a better adaptation for the frequency of the overall system. Accordingly, the frequency control regulates the mechanical power of the wind turbine.

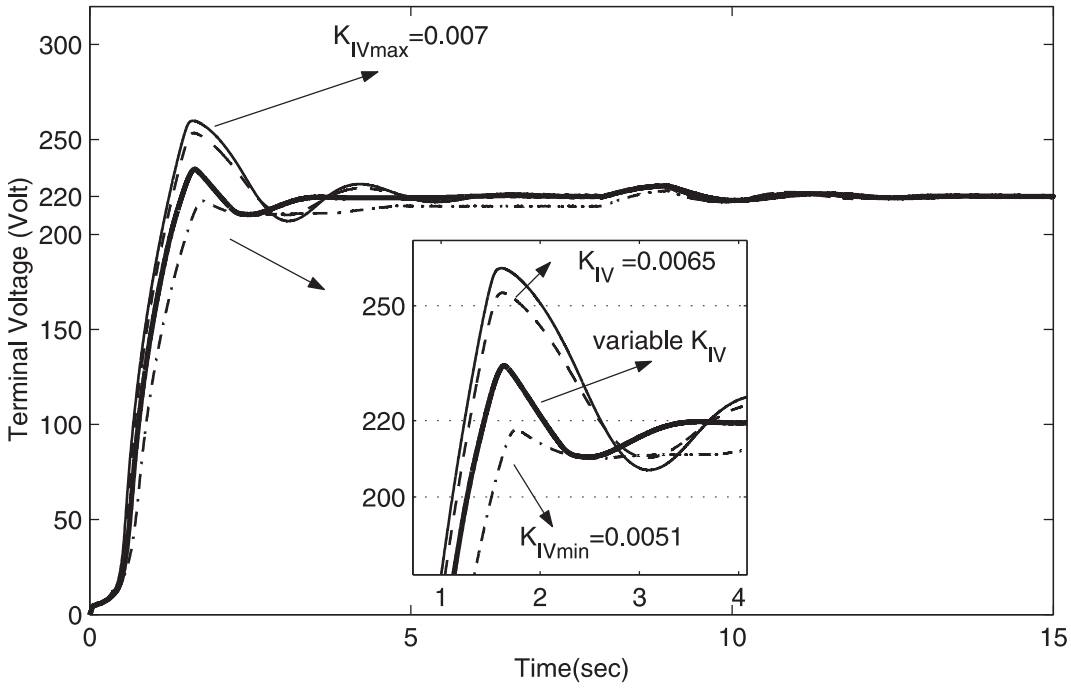

Fig. 3: Dynamic response of the terminal voltage with different values of integral gain for voltage control

4 Controllers

Two different types of controller strategies have been conducted. First, the conventional PI controller with fixed and variable gains is applied. Second, FLC is applied to adjust the value of K_I for both frequency and voltage controllers.

4.1 Conventional PI controller

The simulation program is carried out for different values of K_I while the value of the proportional gain is kept constant, as shown in Fig. 3. It is observed from the simulation results that the value of the percentage overshoot (P.O.S), rising time and settling time change as K_I is changed. Then the technique of having variable KI depending on the voltage error, for voltage control, is introduced to obtain the advantage of high and low value of the integral gain of voltage loop K_{IV}.

4.2 PI-Controller with variable gain

A program has been developed to compute the value of the variable integral gain K_{IV}, using the following rule:

if ($e_V < e_{V\min}$), $K_{IV} = K_{IV\min}$;
elseif ($e_V > e_{V\max}$), $K_{IV} = K_{IV\max}$;
else ($e_{V\min} < e_V < e_{V\max}$),
$M = (K_{IV\max} - K_{IV\min})/(e_{V\max} - e_{V\min})$;
$C = K_{IV\min} - M \times e_{V\min}$;
$K_{IV} = M \times e_V + C$;
end

where, e_V = voltage error, $e_{V\min}$ = minimum value of the voltage error, $e_{V\max}$ = maximum value of the voltage error, $K_{IV\min}$ = minimum value of K_{IV}, $K_{IV\max}$ = maximum value of K_{IV}, C is a constant and M is the slope value. Fig. 4 shows the rule for calculating K_{IV} of K_{IV} against the terminal voltage error e_V. The value of $e_{V\min}$ and $e_{V\max}$ is obtained by trail and error to give the best dynamic performance.

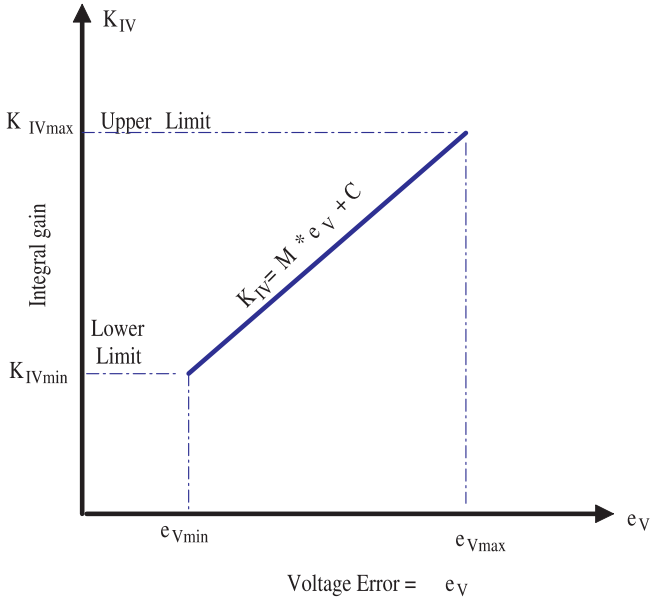

Fig. 4: Variable integral gain for PI controller

The proportional gains (K_{PV} and K_{PF}) are also kept constant for the voltage and frequency controllers, respectively. Various characteristics are tested to study the effect of changing the value of (K_{IV}) to update the voltage control. The simulation results cover the starting period and the period when the system is subjected to a sudden increase in the load, at instant 8 sec. Fig. 3 shows the simulation results for the variable K_{IV}. Figs. 5, 6 show the effect of variable voltage integral gain K_{IV} and frequency K_{IF} controllers versus time, respectively.

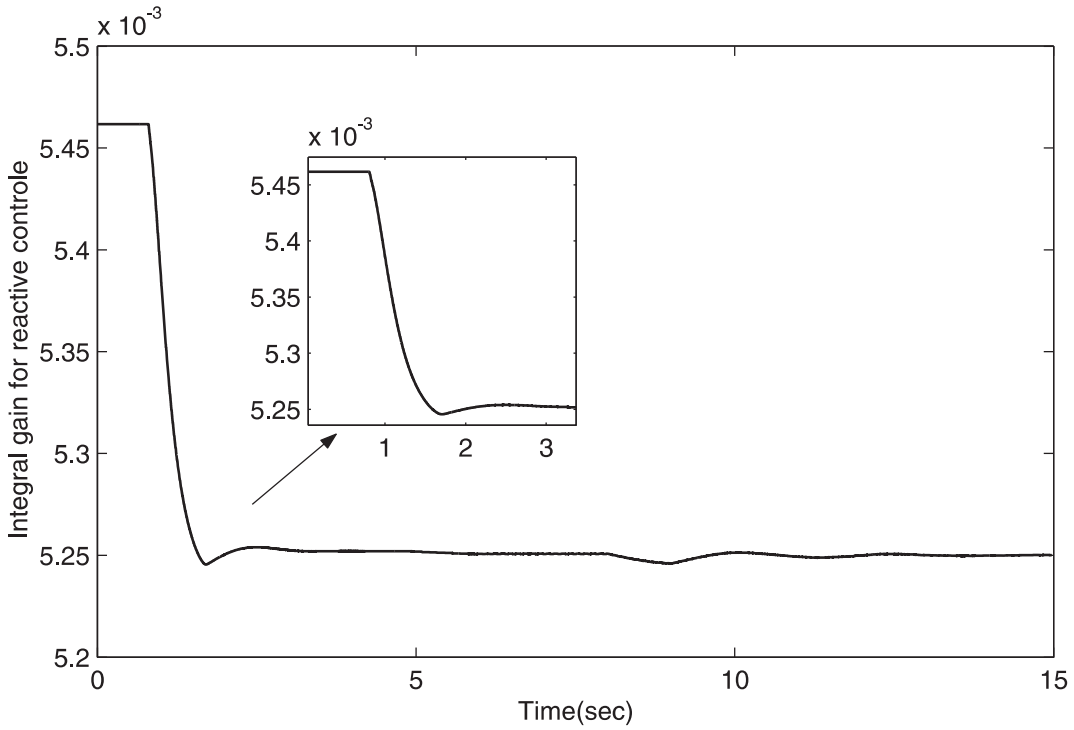

Fig. 5: Variable integral gain in PI-voltage controller with FLC

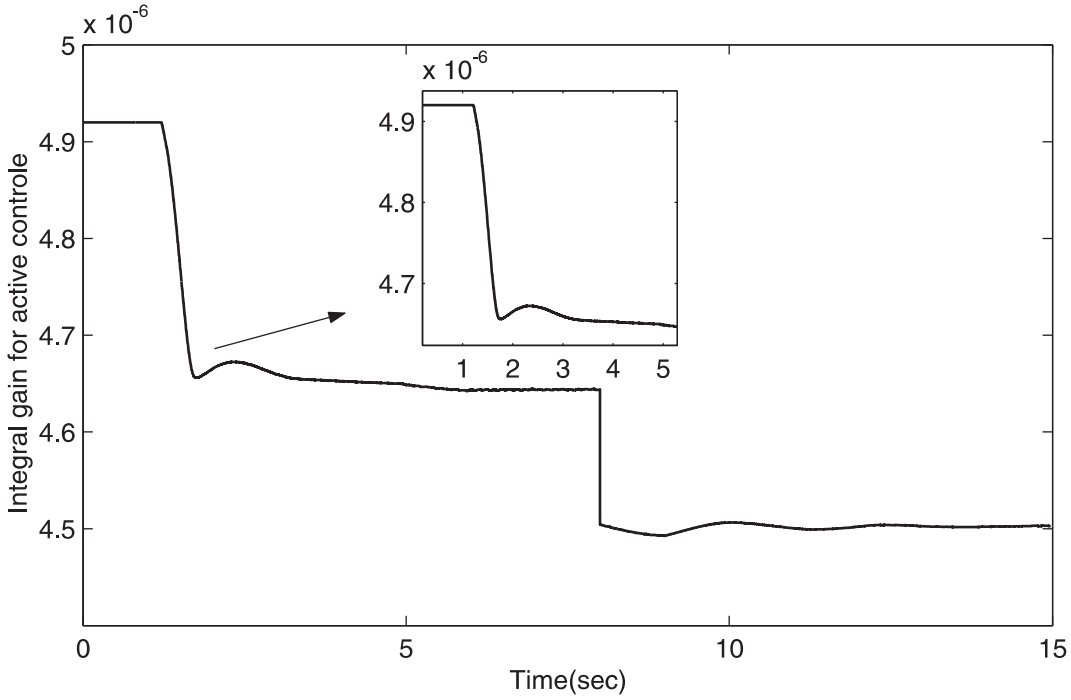

Fig. 6: Variable integral gain in PI-frequency controller with FLC

5 A Fuzzy Logic Controller (FLC)

To design the fuzzy logic controller, FLC, the control engineer must gather information on how the artificial decision maker should act in the closed-loop system, and this would be done from the knowledge base [10]. The fuzzy system is constructed from input fuzzy sets, fuzzy rules and output fuzzy sets, based on the prior knowledge base of the system. Fig. 7 shows the basic construction of the FLC. There are rules to govern and execute the relations between inputs and outputs for the system. Every input and output parameter has a membership function which could be introduced between the limits of these parameters through a universe of discourse. The better the adaptation of the fuzzy set parameters is, the better the tuning of the fuzzy output is conducted. The proposed FLC is used to compute and adapt the variable integral gain K_I of PI controller.

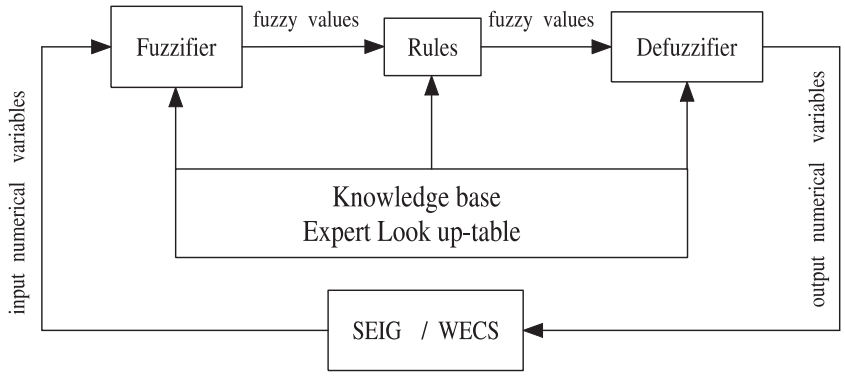

Fig. 7: The three stages of the fuzzy logic controller

5.1 Global input and output variables

For voltage control the fuzzy input vector consists of two variables; the terminal voltage deviation e_V, and the change of the terminal voltage deviation Δe_V. Five linguistic variables are used for each of the input variables, as shown in Fig. 8a and Fig. 8b, respectively. The output variable fuzzy set is shown in Fig. 8c and Fig. 8d, while shows the fuzzy surface. For frequency control, the fuzzy input vector also consists of two variables; the mechanical power deviation e_F, and the change of the mechanical power deviation Δe_F. Five linguistic variables are used for each of the input variables, as shown in Fig. 9a and Fig. 9b, respectively. The output variable fuzzy set is shown in Fig. 9c, and Fig. 9d shows the fuzzy surface. In Figs. 8, 9 linguistic variables have been used for the input variables, P for Positive, N for Negative, AV for Average, B for Big and S for Small. For example, PB is Positive Big and NS is Negative Small, etc. After constructing the fuzzy sets for input

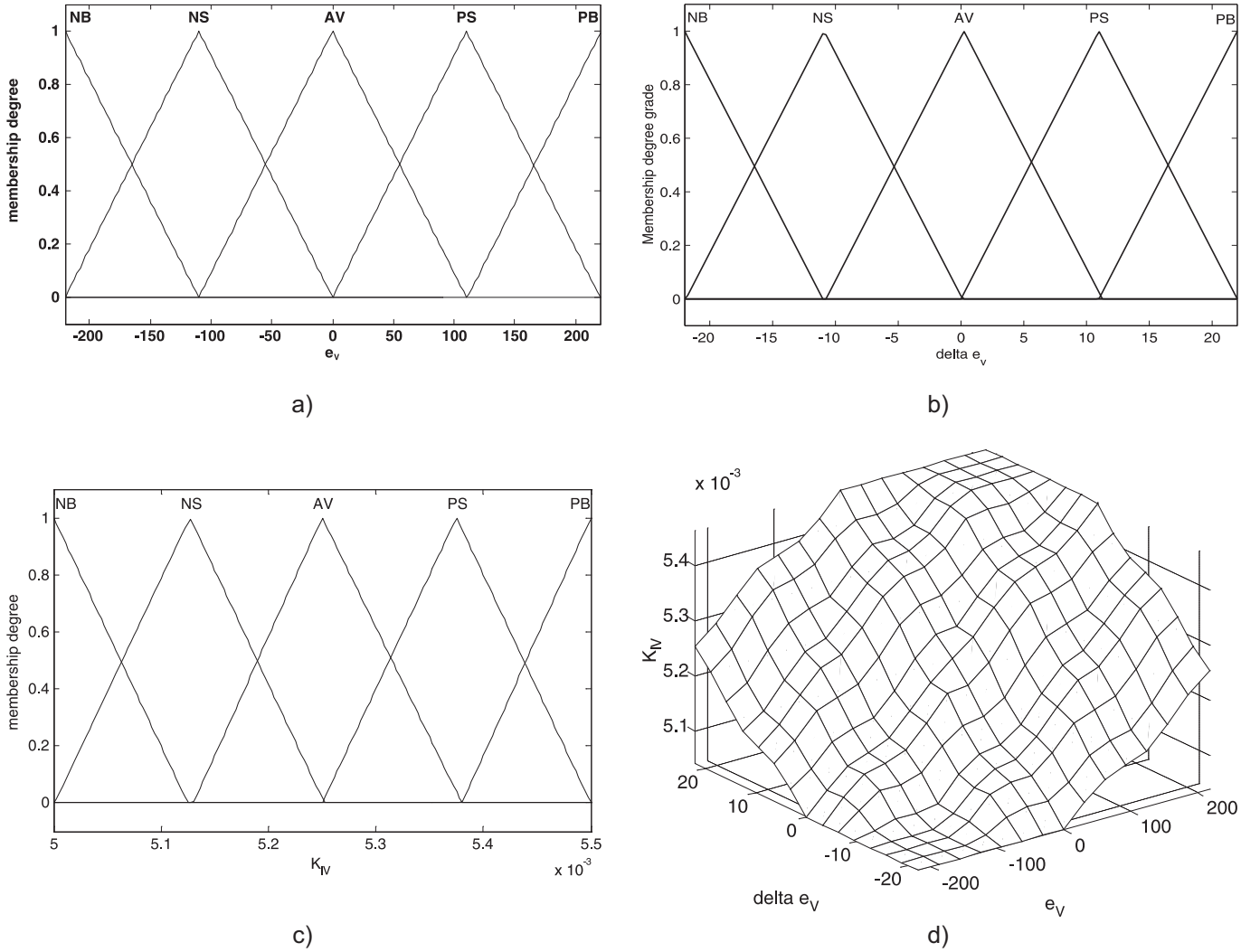

Fig. 8: a) membership function of voltage error, b) membership function of change in voltage error, c) membership function of variable K_{IV}, d) fuzzy surface

and output variables, it is required to develop the set of rules, the so-called Look-up table, which defines the relation between the input variables, e_V, e_F, Δe_V and Δe_F and the output variable of the fuzzy logic controller. The output from the fuzzy controller is the integral gain value of K_I used in the PI controller. The look-up table is given in Table 1.

Table 1: Look up table of fuzzy set rules for voltage control

Voltage Deviation (e_V)	Voltage Deviation Change (Δe_V)				
	NB	NS	AV	PS	PB
NB	NB	NB	NB	NS	AV
NS	NB	NB	NS	AV	PS
AV	NB	NS	AV	PS	PB
PS	NS	AV	PS	PB	PB
PB	AV	PS	PB	PB	PB

5.2 The defuzzification method

The Minimum of maximum method has been used to find the output fuzzy rules representing a polyhedron map, as shown in Fig. 10. First, the minimum membership grade, which is calculated from the minimum value for the intersection of the two input variables (x_1 and x_2) with the related fuzzy set in that rule. This minimum membership grade is calculated to rescale the output rule, then the maximum is taken, as shown in Fig. 11. Finally, the centroid or center of area has been used to compute the fuzzy output, which represents the defuzzification stage, as follows:

$$K_I = \frac{\int y\,\mu(y)\,\mathrm{d}y}{\int \mu(y)\,\mathrm{d}y}.$$

More details about the variables of the above equation are given in [10].

6 Simulation results

6.1 Dynamic performance due to sudden load variation

The FLC utilizes the terminal voltage error (e_V) and its rate of change (Δe_V) as input variables to represent the voltage control. The output of FLC is used to tune up K_I of the PI controller. Another FLC is used to regulate the mechanical power via the blade angle adaptation of the wind turbine. Figs. 8a, b, c and d depict the fuzzy sets of e_V, Δe_V, K_{IV} and the

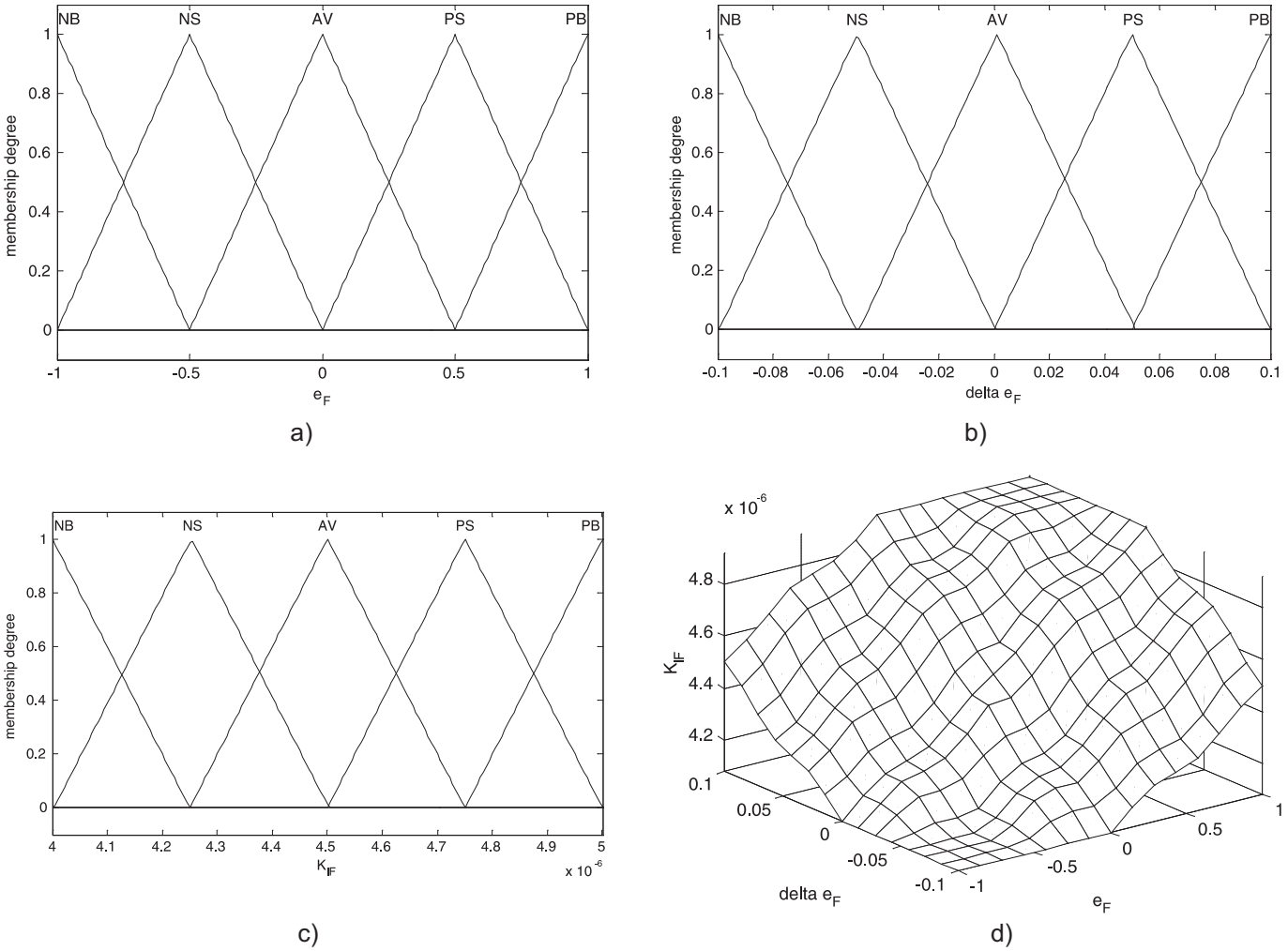

Fig. 9: a) membership function of mech. power error, b) membership function of change on mech. power error, c) membership function of variable K_{IF}, d) fuzzy surface

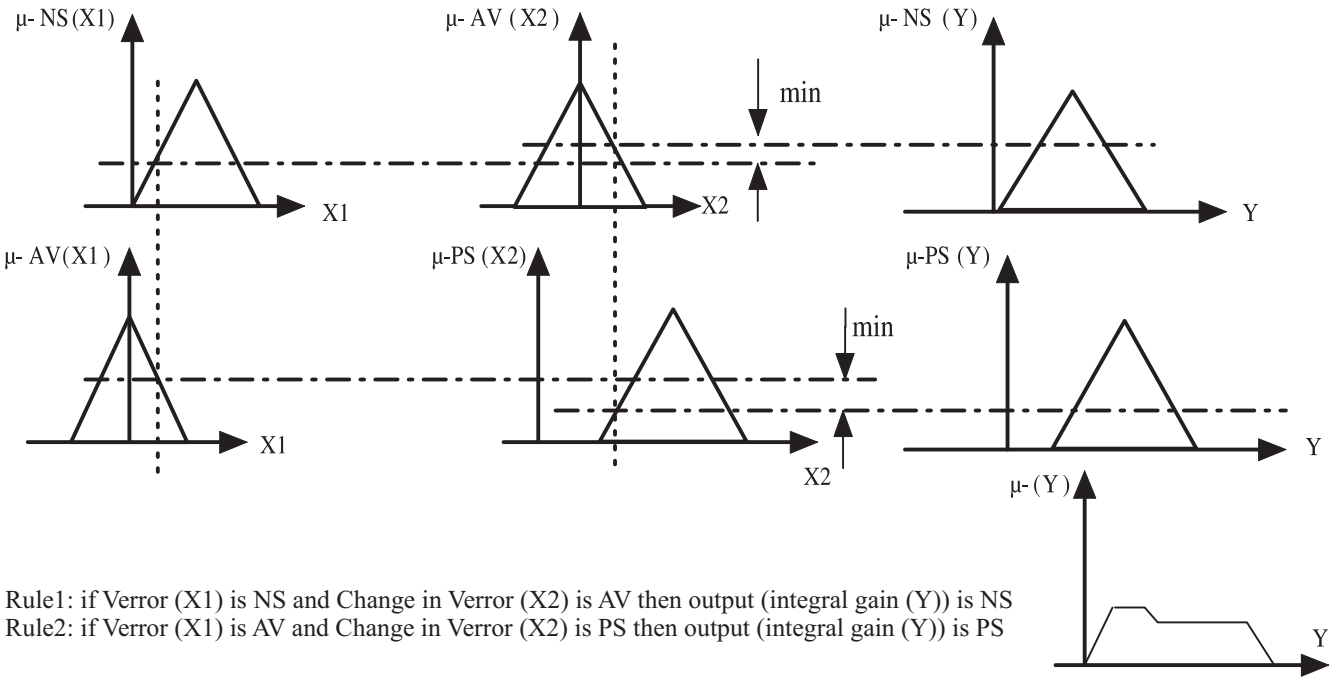

Fig. 10: Schematic diagram of the defuzzification method using the center of area

fuzzy surface, respectively. The terminal voltage error (e_V) varies between (–220 and 220) and its change (Δe_V) varies between (– 22 and 22). The output of FLC is KIV, which changes between (5e–003 and 5.5e–003). Table 1 shows the lookup table of fuzzy set rules for voltage control. The same technique is applied for the frequency controller, where the two inputs for FLC are the mechanical power error (e_F), which varies between (–1 and 1) and its change (Δe_F), which varies between (–0.1 and 0.1). The output of FLC is K_{IF}, which changes between (4e–006 and 5e–006). The output of the PI-FLC in the frequency controller adapts the pitch angle value to enhance the stator frequency. Fig. 9a, b, c and d show the fuzzy sets of e_F, Δe_F, the related output fuzzy set and fuzzy surface, respectively.

Based on the mathematical model of the system, equipped with two controllers (PI & FLC) for terminal voltage and blade angle, the simulation is carried out using the MATLAB- Simulink Package. It runs for a PI controller with varying integral gain finding a relation between the voltage or frequency error and the value of these gains. Figs. 11, 12, 13 show the simulation results for the terminal voltage for different loads. At time = 8 sec the system is subjected to sudden

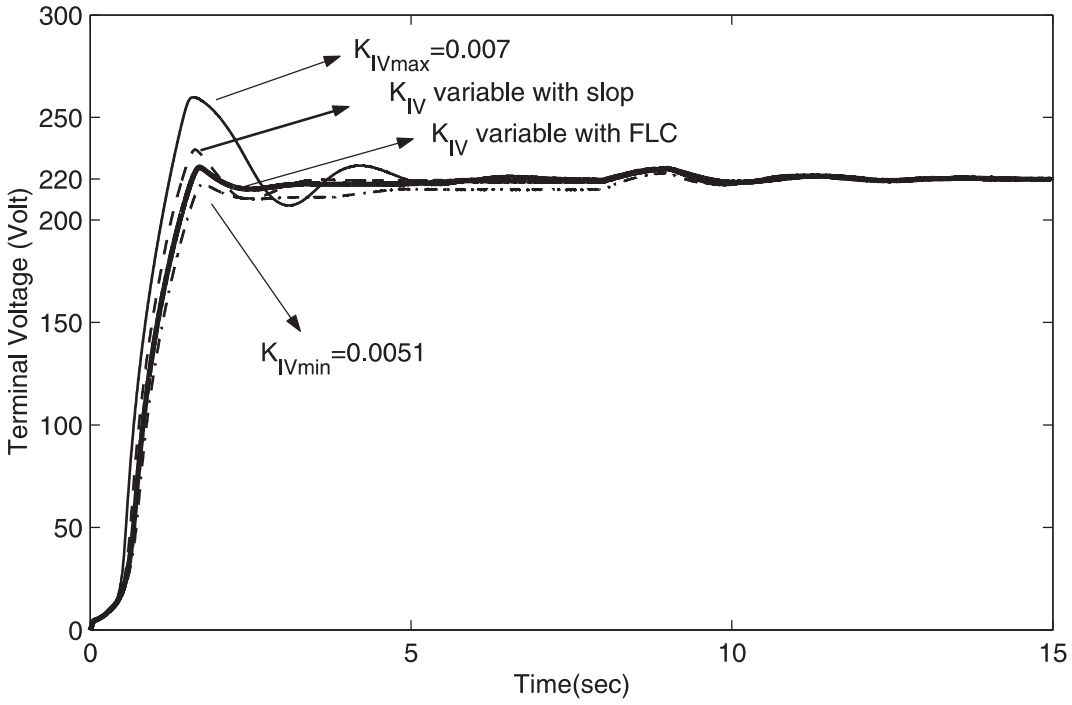

Fig. 11: Dynamic response of terminal voltage for PI with and without FLC

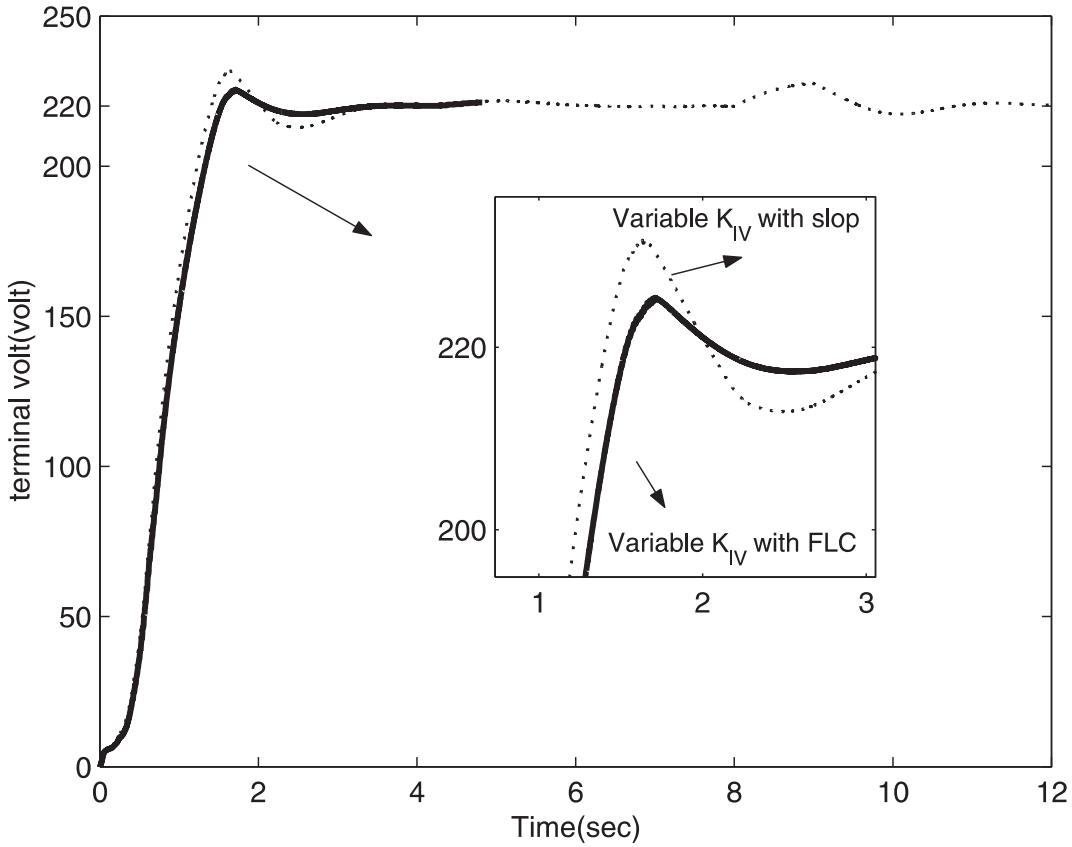

Fig. 12: Dynamic response of terminal voltage for PI with and without FLC

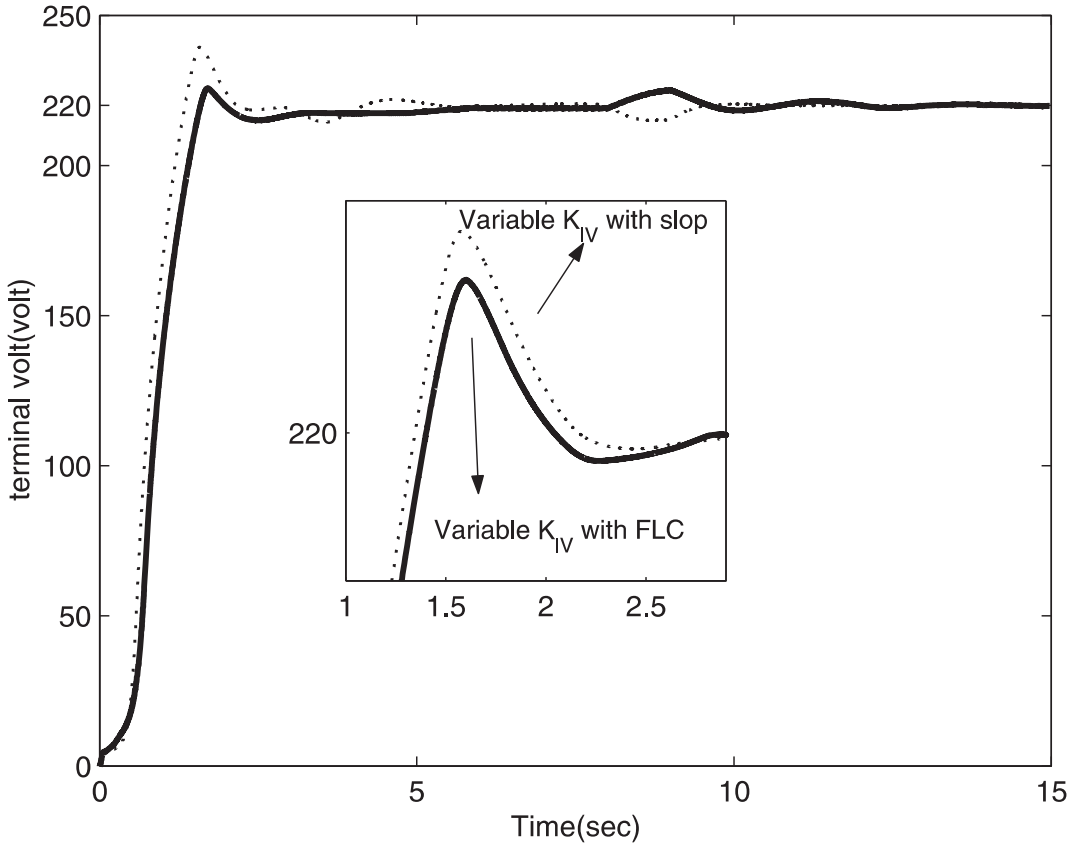

Fig. 13: Dynamic response of terminal voltage for PI with and without FLC

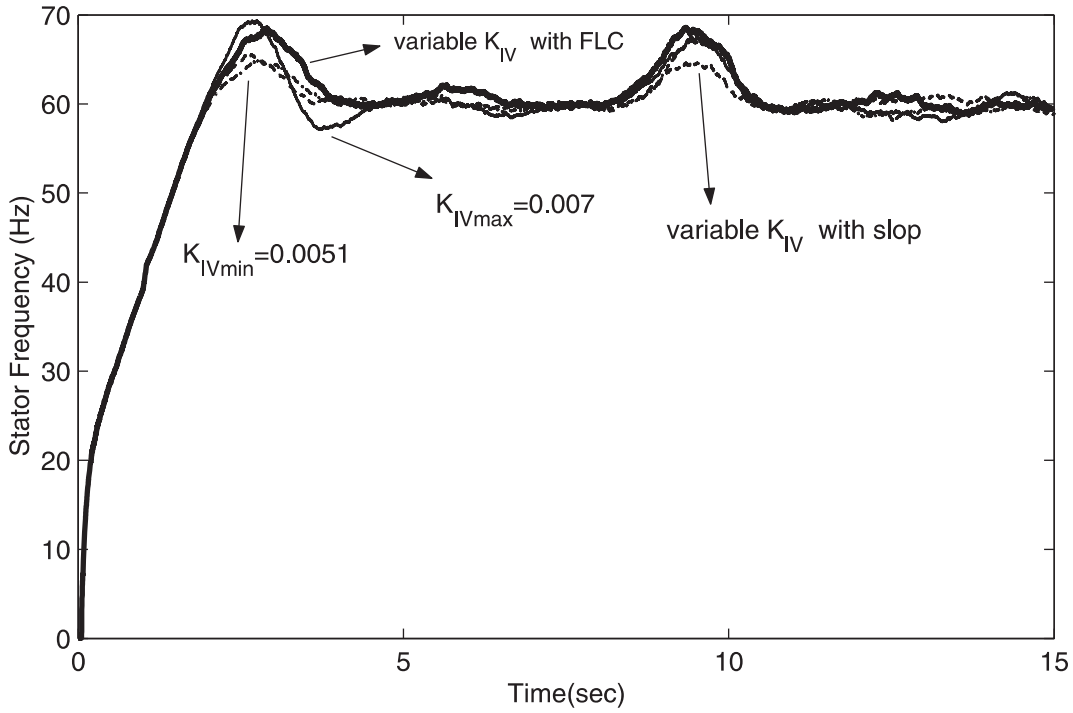

Fig. 14: Dynamic response of stator frequency for PI with and without FLC

change in load. Fig. 14 shows the stator frequency. The system is equipped with a conventional controller having fixed and variable integral gain and the FLC algorithm. The proposed FLC is used to adapt K_I to give a better dynamic performance for the overall system, as shown in Figs. 11, 12, 13, regarding P.O.S and settling time compared with fixed PI and PI with variable K_I for different loads. Figs. 15, 16 depict the simulation results for the load current and controller's duty cycle. The same conclusion is achieved as explained for Fig. 11.

6.2 Dynamic performance due to sudden wind speed variation

There are different simulation results when the overall system is subjected to a suddenly disturbance the wind speed from 7 m/s to 15 m/s in Figs. 17, 18 show the simulation results of the wind speed variation and the stator frequency, respectively. The simulation given in Fig. 18 shows the ability of the

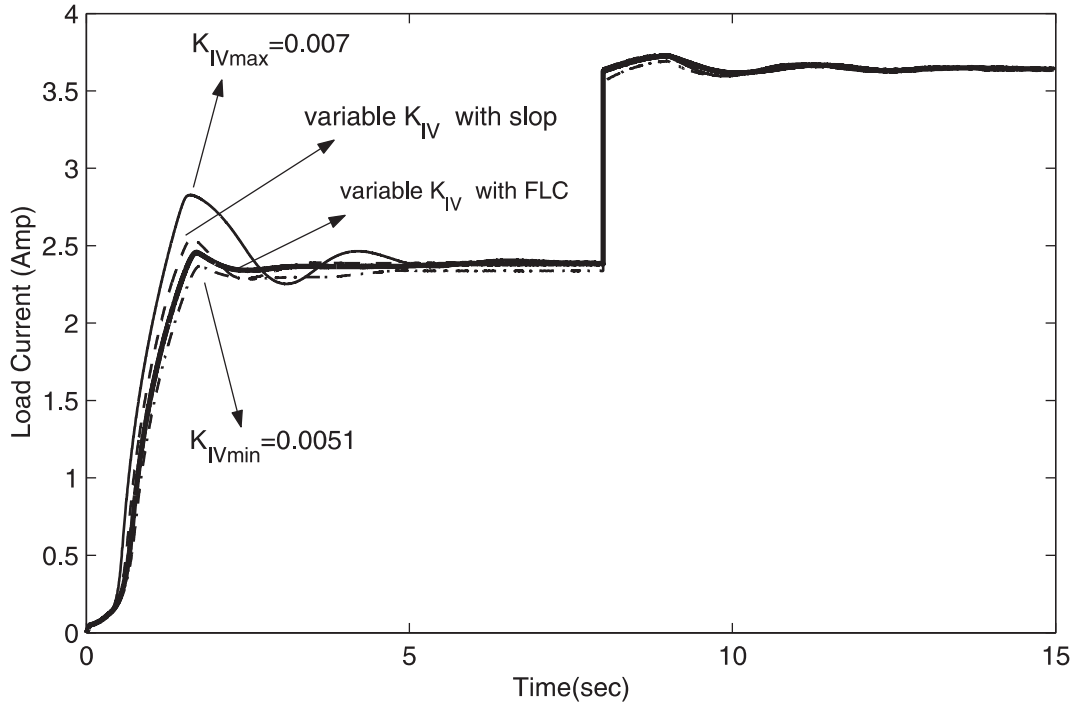

Fig. 15: Dynamic response of load current for PI with and without FLC

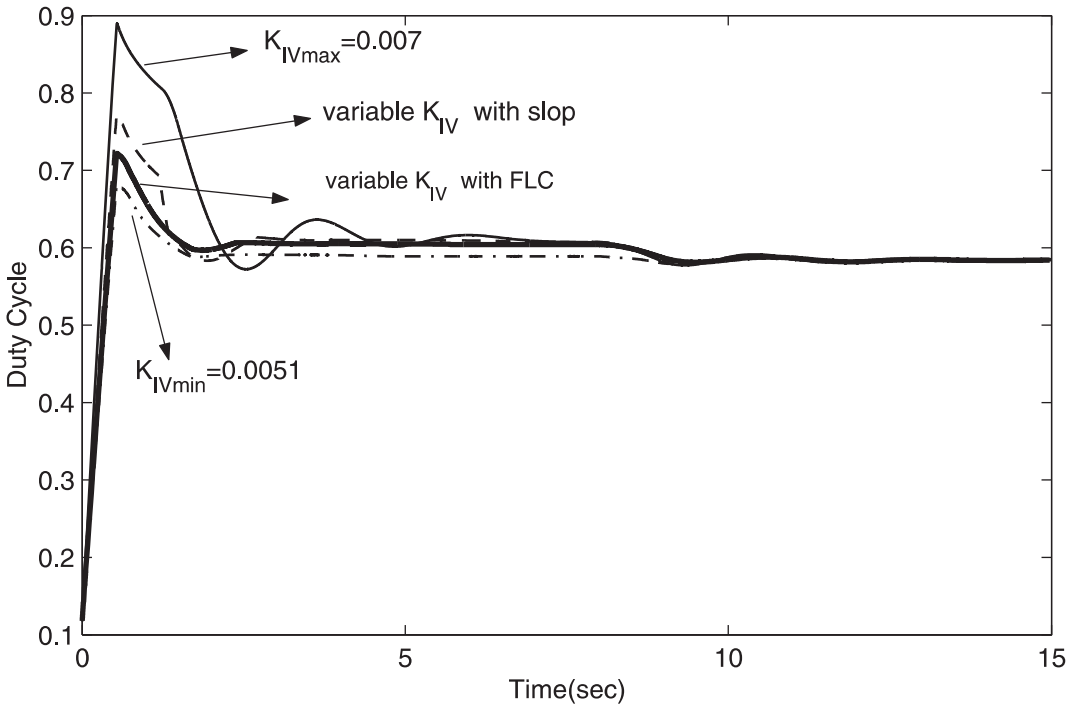

Fig. 16: Dynamic response of duty cycle for PI with and without FLC

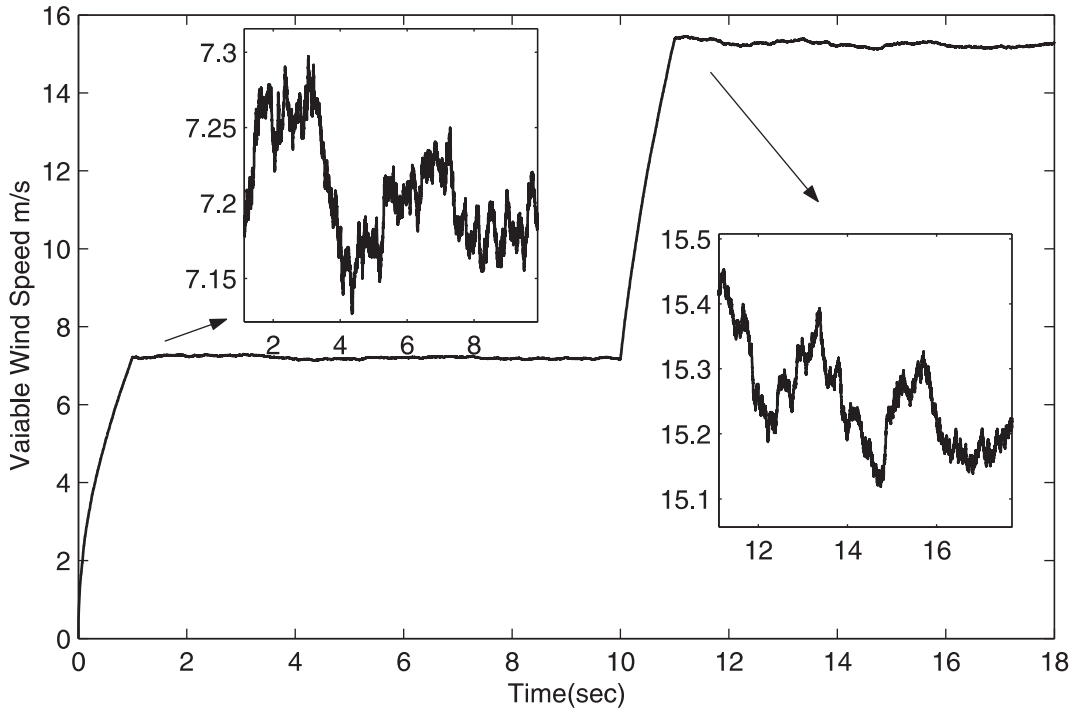

Fig. 17: Suddenly variation for the wind speed versus time

proposed controller to overcome the speed variation for variable and fixed integral gain.

7 Conclusion

This paper presents an application of FLC to a self-excited induction generator driven by wind energy. The proposed FLC is applied to frequency and voltage controls of the system to enhance its dynamic performance. FLC is used to regulate the duty cycle of the switched capacitor bank to adjust the terminal voltage of the induction generator. FLC is also applied to regulate the blade angle of the wind energy turbine to control the stator frequency of the overall system. The simulation results show better dynamic performance of the overall system using the FLC controller than for the variable PI type. Another simulation was conducted to study the dynamic performance to this system with a suddenly disturbance for wind speed variation. A comparison was conducted for the stator frequency in dynamic performance with variable and fixed K_I.

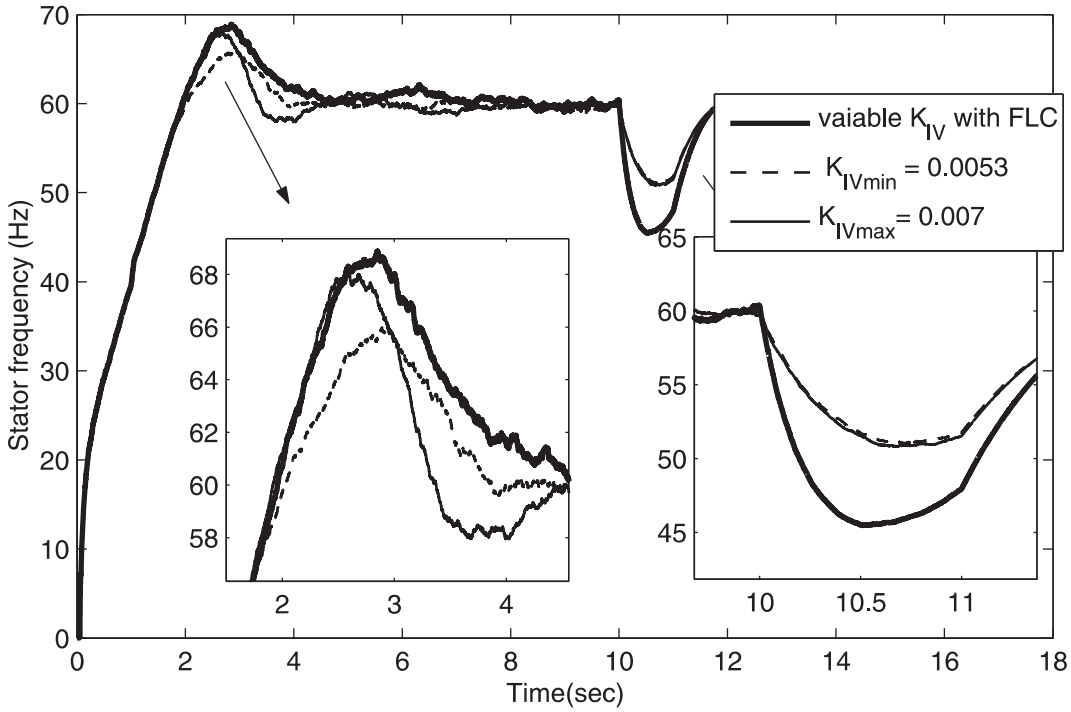

Fig. 18: Stator Frequency according to the wind speed variation for SEIG controlled by FLC & PI

Appendix

SEIG differential equations at no load

v_{ds} Stator Voltage (volt) Differential Equation at Direct Axis

$$v_{ds} = -R_s \cdot i_{ds} - \left(\frac{\omega}{\omega_b}\right)\varphi_{qs} + p\left(\frac{\varphi_{ds}}{\omega_b}\right), \tag{1}$$

v_{qs} Stator Voltage Differential Equation at Quadrate Axis

$$v_{qs} = -R_s \cdot i_{qs} - \left(\frac{\omega}{\omega_b}\right)\varphi_{ds} + p\left(\frac{\varphi_{qs}}{\omega_b}\right), \tag{2}$$

v_{dr} Rotor Voltage Differential Equation at Direct Axis

$$v_{dr} = R_r \cdot i_{dr} - \left(\frac{(\omega - \omega_r)}{\omega_b}\right)\varphi_{qr} + p\left(\frac{\varphi_{dr}}{\omega_b}\right), \tag{3}$$

v_{qr} Rotor Voltage Differential Equation at Quadrate Axis

$$v_{qr} = R_r \cdot i_{qr} - \left(\frac{(\omega - \omega_r)}{\omega_b}\right)\varphi_{dr} + p\left(\frac{\varphi_{qr}}{\omega_b}\right), \tag{4}$$

where

p is the differentiation parameter d/dt.

Flux Linkage Differential Equation for Stator and Rotor components

$$\varphi_{ds} = -X_{ls} \cdot i_{ds} + x_m(i_{dr} - i_{ds}), \tag{5}$$

where

φ_{ds} is the stator flux linkage (Wb) at direct axis,

i_{dr} the rotor current (A) at direct axis,

i_{ds} the stator current (A) at direct axis.

$$\varphi_{qs} = -X_{ls} \cdot i_{qs} + x_m(i_{qr} - i_{qs}), \tag{6}$$

where

φ_{qs} is the stator flux linkage at quadrant axis,

i_{qr} the rotor current at quadrant axis,

i_{qs} the stator current at the quadrant axis.

$$\varphi_{dr} = X_{lr} \cdot i_{dr} + x_m(i_{dr} - i_{ds}), \tag{7}$$

$$\varphi_{qr} = X_{lr} \cdot i_{qr} + x_m(i_{qr} - i_{qs}), \tag{8}$$

$$\frac{d\varphi_{qs}}{dt} = \omega_b \cdot (v_{qs} + R_s \cdot i_{qs} - \varphi_{ds}), \tag{9}$$

$$\frac{d\varphi_{ds}}{dt} = \omega_b \cdot (v_{ds} + R_s \cdot i_{ds} - \varphi_{qs}), \tag{10}$$

where

φ_{dr}, φ_{qr} is the rotor flux linkage at the direct and quadrant axis, respectively,

w_b the base speed.

Magnetizing reactance and load case differential equations

$$i_{ds} = \left(c \cdot \left(\frac{dv_{ds}}{dt}\right)\right) + \frac{v_{ds} - L_L\left(\frac{di_{Lds}}{dt}\right)}{R_L}, \tag{11}$$

$$i_{qs} = \left(c \cdot \left(\frac{dv_{qs}}{dt}\right)\right) + \frac{v_{qs} - L_L\left(\frac{di_{Lqs}}{dt}\right)}{R_L}, \tag{12}$$

$$i_m = \left((i_{qr} - i_{qs})^2 + (i_{dr} - i_{ds})^2\right)^{0.5}, \tag{13}$$

$$T_e = \lfloor \varphi_{ds} \cdot i_{qs} - \varphi_{qs} \cdot i_{ds} \rfloor, \tag{14}$$

$$x_m = 105.77 \quad \ldots . \text{at} \quad 0.0 \le i_m < 0.864, \tag{15}$$

$$x_m = \frac{340.2}{i_m + 2.35} \quad \ldots . \text{at} \quad 0.864 \le i_m < 1.051, \tag{16}$$

$$x_{\mathrm{m}} = \frac{227.4}{i_{\mathrm{m}} + 1.22} \ldots\ldots \text{at } 1.051 \le i_{\mathrm{m}} < 1.476, \quad (17)$$

$$x_{\mathrm{m}} = \frac{202.3}{i_{\mathrm{m}} + 9.3} \ldots\ldots \text{at } 1.476 \le i_{\mathrm{m}} < 1.717, \quad (18)$$

$$x_{\mathrm{m}} = \frac{179.8}{i_{\mathrm{m}} + 6.3} \ldots\ldots \text{at } 1.717 \le i_{\mathrm{m}}. \quad (19)$$

Excitation differential equations

$$i_{\mathrm{cd}} = (c * p * v_{\mathrm{cd}} - \omega_{\mathrm{s}} * C * v_{\mathrm{cq}}), \quad (20)$$

$$i_{\mathrm{cd}} = (c * p * v_{\mathrm{cd}} - \omega_{\mathrm{s}} * C * v_{\mathrm{cq}}), \quad (21)$$

where

ω_{s} is the synchronous speed (rad/sec),
i_{cd} the capacitor current in the direct axis,
i_{cq} the capacitor current in the quadrant axis,
C the value of the capacitor bank.

$$\left(C * \frac{\mathrm{d}v_{\mathrm{ds}}}{\mathrm{d}t}\right) = (i_{\mathrm{ds}} - i_{\mathrm{Lds}}), \quad (22)$$

$$\left(C * \frac{\mathrm{d}v_{\mathrm{qs}}}{\mathrm{d}t}\right) = (i_{\mathrm{qs}} - i_{\mathrm{Lqs}}), \quad (23)$$

$$(L_{\mathrm{L}} * p i_{\mathrm{Lds}}) = (v_{\mathrm{ds}} - R_{\mathrm{L}}\, i_{\mathrm{Lds}}), \quad (24)$$

$$(L_{\mathrm{L}} * p i_{\mathrm{Lqs}}) = (v_{\mathrm{qs}} - R_{\mathrm{L}}\, i_{\mathrm{Lqs}}), \quad (25)$$

$$\left(C * \frac{\mathrm{d}v_{\mathrm{ds}}}{\mathrm{d}t}\right) = i_{\mathrm{ds}} - \frac{v_{\mathrm{ds}} - \left(L_{\mathrm{L}} * \frac{\mathrm{d}i_{\mathrm{Lds}}}{\mathrm{d}t}\right)}{R_{\mathrm{L}}}, \quad (26)$$

$$\left(C * \frac{\mathrm{d}v_{\mathrm{qs}}}{\mathrm{d}t}\right) = i_{\mathrm{qs}} - \frac{v_{\mathrm{qs}} - \left(L_{\mathrm{L}} * \frac{\mathrm{d}i_{\mathrm{Lqs}}}{\mathrm{d}t}\right)}{R_{\mathrm{L}}}, \quad (27)$$

where

i_{Lds} is the load current in the direct axis,
i_{Lqs} the load current in quadrant axis,
R_{L} the load resistance (Ω),
L_{L} the load inductance (H).

$$C_{\mathrm{eff}} = \frac{C_{\max}}{(1-\lambda)^2 + \sigma(\lambda)^2}, \quad (28)$$

where

C_{eff} is the effective capacitor bank value (μF),
$C_{\max}$ is the maximum capacitor value,
$C_{\min}$ is the minimum capacitor value,
$\sigma = (C_{\max}/C\min)$, and λ is the duty cycle value.

Mechanical differential equations

$$\frac{\mathrm{d}\omega_{\mathrm{r}}}{\mathrm{d}t} = \frac{\omega_{\mathrm{b}}}{2H}(T_{\mathrm{m}} - T_{\mathrm{e}} - B \cdot \omega_{\mathrm{r}}), \quad (29)$$

where ω_{r} is the rotor speed (rad/sec).

$$P_{\mathrm{m}} = \frac{1}{8}\pi\, \rho\, C_{\mathrm{p}}\, D^2\, v_{\mathrm{w}}^3, \quad (30)$$

$$\omega_{\mathrm{m}} = \frac{2\pi\, n}{60}, \quad (31)$$

$$T_{\mathrm{m}} = \frac{P_{\mathrm{m}}}{\omega_{\mathrm{m}}}, \quad (32)$$

$$C_p = (0.44 - 0.0167\beta) \cdot \sin\frac{\pi(\mu - 3)}{15 - 0.3 * \beta} - 0.00184(\mu - 3)\beta, \quad (33)$$

$$\mu = \omega_m \frac{R}{v_w} = \frac{D\,\pi\, n}{60 v_w}, \quad (34)$$

$$\frac{\mathrm{d}\omega_{\mathrm{r}}}{\mathrm{d}t} = \frac{\omega_{\mathrm{b}}}{2H}(T_{\mathrm{m}} - T_{\mathrm{e}} - B_{\mathrm{a}} \cdot \omega_{\mathrm{r}}), \quad (35)$$

where

ω_{m} is the mechanical speed (rad/sec),
P_{m} the mechanical power (kW),
T_{m} the mechanical torque (Nm),
n the rotor revolution per minute (rpm),
C_{p} the power coefficient of the wind turbine,
β the blade pitch angle (°),
μ the tip speed ratio,
v_{w} the wind speed (m/s),
R the rotor radius of the wind turbine (m),
D the rotor diameter of the wind turbine (m),
B_{a} the friction factor,
T_{e} the electrical torque (Nm),
$\pi = 3.14$,
ρ air density (kg/m^3).

References

[1] El-Sousy, F., Orabi, M., Godah, H.: *Indirect Field Orientation Control of Self-Excited Induction Generator for Wind Energy Conversion*. ICIT, December 2004.

[2] Mashaly, A., Sharaf, M. Mansour, M., Abd-Satar, A.A.: A Fuzzy Logic Controller for Wind Energy Utilization Scheme. *Proceedings of the 3rd IEEE Conference of Control Application*, August 24-26, 1994, Glasgow, Scotland, UK.

[3] Li, Wang, Yi-Su, Jian: Dynamic Performance of An Isolated Self Excited Induction Generator Under Various Loading Conditions. *IEEE Transactions on Energy Conversion*, Vol. **15** (1999), No. 1, March 1999, p. 93–100.

[4] Li, Wang, Ching- Huei, Lee: Long- Shunt and Short-Shunt Connections on Dynamic Performance of a SEIG Feeding an Induction Motor Load. *IEEE Transactions on Energy Conversion*, Vol. **14** (2000), No. 1, p. 1–7.

[5] Atallah, A. M., Adel, A.: Terminal Voltage Control of Slef Excited Induction Generators. *Sixth Middle-East Power Systems Conference MEPCON'98*, Mansoura, Egypt, December 15–17,1998, p. 110–118.

[6] Marduchus, C.: *Switched Capacitor Circuits for Reactive Power Generation*. Ph.D. Thesis, Brunuel University, 1983.

[7] Soliman, H. F., Attia, A. F., Mokhymar, S. M., Badr, M.A.L., Ahmed, A. E. M. S.: Dynamic Performance Enhancement of Self Excited Induction Generator Driven by Wind Energy Using ANN Controllers. *Sci. Bull.* Fac. Eng. Ain Shams University, Part II. Vol. 39, No. 2, June 30, 2004, p. 631–651, ISSN 1110-1385.

[8] Mokhymar S. M: Enhancement of The Performance of Wind Driven Induction Generators Using Artificial Intelligence Control. Ph.D. thesis Fac. Eng. Ain Shams University, March. 10, 2005.

[9] Ezzeldin, S. A., Xu, W.: Control Design and Dynamic Performance Analysis of a Wind Turbine- Induction Generator Unit. *IEEE Transaction on Energy Conversion*, Vol. **15** (2000), No. 1, March 2000, p. 91–96.

[10] Passino, K. M., Yurkovich, S.: *Fuzzy Control, Library of Congress Cataloging-in-Publication Data*. (Includes bibliographical references and index). Addison Wesley Longman, Inc., 1998, ISBN 0-201-18074-X.

Associate Prof. Dr. Ing. Hussein F. Soliman
e-mail: hfaridsoliman@yahoo.com

Currently Elect. & Computer Department
King Abdulaziz University
Faculty of Engineering
Jeddah, Saudi Arabia

Dr. Ing. Abdel-Fattah Attia
e-mail: attiaa1@yahoo.com

National Research Inst. of Astronomy and Geophysics
P.O. 11421 Helwan
Cairo, Egypt

Dr. Ing. Mokhymar M. Sabry
e-mail: sabry40@hotmail.com

Electricity & Energy Ministry
New & Renewable Energy Authority, Wind Management
Cairo, Egypt

Prof. Dr. Ing. M. A. L. Badr

Elect. Power and Machines Department
Ain Shams University
Faculty of Engineering
Abbasia
Cairo, Egypt

